BMC Cancer

RESEARCH

Open Access

A novel serum protein biomarker for the late-stage diagnosis of nasopharyngeal carcinoma

Yi-Xi Pan[1†], Qi Huang[2†], Shan Xing[2*] and Qian-Ying Zhu[1*]

Abstract

Background Nasopharyngeal carcinoma (NPC) is a malignant tumor prevalent in Southern China, strongly associated with Epstein-Barr virus (EBV) infection. Accurate diagnosis is critical in determining treatment strategies for NPC. In clinical practice, imaging techniques are the most predominant diagnostic methods, which are costly and may fail to detect small metastatic lesions. Moreover, while EBV antibody and DNA tests contribute to the assessment of tumor progression, they carry the risk of false negatives.

Methods To develop novel serum protein biomarkers for late-stage NPC diagnosis, our study included 189 samples, including healthy controls (HCs) and early- or late-stage NPC patients. A high-throughput serum proteomics approach was employed to delineate protein profiles, followed by enzyme-linked immunosorbent assay (ELISA) validation of candidate biomarkers.

Results Our study identified fibronectin 1 (FN1) as a promising serum biomarker for late-stage NPC. The serum levels of FN1 significantly decreased with tumor progression, achieving AUCs of 0.71 and 0.72 in differentiating late-stage NPC patients from HCs and early-stage NPC patients, respectively. Importantly, FN1 demonstrated diagnostic utility in challenging cases, accurately identifying all VCA-IgA-negative and 88.2% EBV DNA-negative patients with late-stage NPC. Combining FN1 with VCA-IgA or EBV DNA test significantly increased diagnostic sensitivity for advanced NPC.

Conclusions Our discovery of FN1 as a biomarker for the late-stage diagnosis of NPC will assist in clinical treatment decisions and improve the prognosis of patients.

Keywords Nasopharyngeal carcinoma, Fibronectin 1, Biomarker, Diagnosis

Introduction

Nasopharyngeal carcinoma (NPC) is one of the most common malignancies of the head and neck, mainly occurring in the parietal and lateral walls of the nasopharynx, particularly in the pharyngeal recess [1]. In Southern China, NPC is a significant health burden, with an annual incidence as high as 30–80 per 100,000 individuals [2]. The occurrence of NPC is widely accepted to be linked primarily to Epstein-Barr virus (EBV) infection, with nearly 97% of patients worldwide being EBV-positive [3, 4]. Additionally, genetic predispositions and unhealthy lifestyle habits, such as heavy smoking and the

†Yi-Xi Pan and Qi Huang contributed equally to this work.

*Correspondence:
Shan Xing
Xingshan@sysucc.org.cn
Qian-Ying Zhu
zhuqy37@mail.sysu.edu.cn
[1] Department of Laboratory Medicine, The Eighth Affiliated Hospital, Sun Yat-Sen University, Shenzhen 518033, China
[2] Department of Clinical Laboratory, State Key Laboratory of Oncology in South China, Guangdong Key Laboratory of Nasopharyngeal Carcinoma Diagnosis and Therapy, Sun Yat-Sen University Cancer Center, Guangzhou 510060, China

consumption of salted foods can also contribute to NPC [5, 6].

Notably, early-stage NPC responds well to radiotherapy, with a high 5-year survival rate up to 90% [7–9]. However, ~ 76% of patients are diagnosed at a late stage, and an additional 5% present with distant metastatic lesions at initial diagnosis. Moreover, ~ 29% of patients with locoregionally advanced stage will experience recurrence posttreatment, with a significantly reduced median survival time of approximately 20 months [10, 11]. Due to the fact that late-stage NPC patients often require multimodal treatment strategies, which can significantly impact their quality of life. Therefore, the accurate identification of late-stage patients is crucial for tailoring therapeutic approaches that may improve patient outcomes and increase survival rates.

Clinically, the identification of NPC mainly depends on biopsy, imaging, and hematological testing. Endoscopic biopsy is the gold standard for confirming the primary cancer. Magnetic resonance imaging (MRI) provides superior recognition of deep tumor infiltration [12]. Positron emission tomography-computed tomography (PET-CT) is particularly advantageous for diagnosing cervical lymph nodes and distant metastases [13, 14]. However, these modalities have inherent limitations, such as the invasiveness of endoscopy, the high costs and time-consuming nature of imaging, and the inapplicability for patients with metallic implants or those who suffer from claustrophobia [15–17]. As a routine population screening indicator, VCA-IgA titer levels vary with tumor progression or recovery, but may be negative in NPC patients [18, 19]. The plasma EBV DNA copy number has high sensitivity and specificity of 97.1% and 98.6%, respectively, for the diagnosis of NPC [20]. A previous study suggested that the rate of EBV DNA positivity is 56.4% in patients with locoregional recurrence and 93.9% in those with distant metastasis [21]. However, there is a lack of standardization in EBV DNA testing protocols, including detection equipment, DNA extraction methods, targeted DNA fragments, quality control, and particularly the determination of thresholds, which still remains contentious issues [22]. Given the pitfalls of current diagnostic methods, the sole reliance on existing surveillance strategies is insufficient to evaluate tumor progression in NPC. There is an urgent need for the development of more accurate and noninvasive biomarkers in the clinic.

In this study, we employed a phased strategy to develop novel serum protein biomarkers for the late-stage diagnosis of NPC. We also evaluated the diagnostic performance of the identified biomarker in combination with VCA-IgA and EBV DNA. This discovery offers a complementary biomarker to current methods, potentially driving future advancements in NPC research.

Methods

Patients and HCs

The Institution Review Board of Sun Yat-sen University Cancer Center (SYSUCC) approved this study. A total of 150 NPC patients and 39 healthy controls (HCs) were enrolled from January 2019 to April 2023 at SYSUCC (Guangzhou, China). We classified stage I and II patients as early-stage nasopharyngeal carcinoma (ENPC) patients, and stage III and IV patients as late-stage nasopharyngeal carcinoma (LNPC) patients.

Sample preparation

Blood samples were centrifuged at 1500 × g at room temperature for 10 min to separate the serum, which was then stored at −80 °C. Initially, the serum samples were centrifuged at 12,000 × g at 4 °C for 10 min to remove cellular debris. The supernatant was subsequently transferred to fresh centrifuge tubes. The depletion of the 14 most abundant proteins was achieved using the Pierce™ Top 14 Abundant Protein Depletion Spin Columns Kit (Thermo Fisher), and the protein concentrations were determined using a BCA kit following the manufacturer's protocol.

Proteins were reduced with 5 mM dithiothreitol at 56 °C for 30 min and alkylated with 11 mM iodoacetamide in the dark at room temperature for 15 min. Following alkylation, the samples were transferred to ultrafiltration tubes for filter-aided sample preparation (FASP) digestion, and were washed by successive replacement with 8 M urea for three cycles at 12,000 × g and room temperature for 20 min each, followed by three cycles with 200 mM TEAB [23]. Trypsin was added at a 1:50 enzyme-to-substrate mass ratio, and the mixture was incubated overnight for digestion. Peptides were recovered by centrifugation at 12,000 × g for 10 min at room temperature, and this step was repeated twice. Finally, the combined peptides were desalted using a Strata X SPE column.

LC–MS/MS analysis

Tryptic peptides were dissolved in Solvent A and directly loaded onto a homemade reversed-phase analytical column (25 cm in length, 100 μm inner diameter). The mobile phase was composed of Solvent A (0.1% formic acid, 2% acetonitrile in water) and Solvent B (0.1% formic acid, 90% acetonitrile in water). Peptides were separated using the following gradient: 0–68 min, 4–20% B; 68–82 min, 20–32% B; 82–86 min, 32–80% B; 86–90 min, 80% B, all at a constant flow rate of 500 nl/min on an EASY-nLC 1200 UPLC system (Thermo Fisher Scientific). The separated peptides were analyzed in an Orbitrap Exploris 480 mass spectrometer equipped with a nano-electrospray ion source. The electrospray voltage

was set to 2300 V, and the FAIMS compensation voltage was adjusted to −70 V and −45 V. Precursors and fragments were analyzed in the Orbitrap detector. The full MS scan resolution was set to 60,000 with a scan range of 400–1200 m/z. The MS/MS scan was set with a fixed first mass of 110 m/z at a resolution of 30,000, with TurboTMT disabled. Up to 15 of the most abundant precursors were selected for further MS/MS analysis with a 30-s dynamic exclusion window. HCD fragmentation was performed using a normalized collision energy (NCE) of 27%. The automatic gain control (AGC) target was set to 75%, with an intensity threshold of 10,000 ions/s and a maximum injection time of 100 ms.

Database search

The resulting MS/MS data were processed using the Proteome Discoverer search engine (version 2.4). Tandem mass spectra were searched against the Homo_sapiens_9606_PR_20230103.fasta database (81,837 entries), concatenated with a reverse decoy and a contaminant database. Trypsin was set as the cleavage enzyme, allowing for up to 2 missed cleavages. The minimum peptide length was set to 6, and the maximum number of modifications per peptide was set to 3. The mass tolerances were set to 10 ppm for precursor ions and 0.02 Da forfragment ions. Carbamido-methylation of cysteine was specified as a fixed modification, whereas oxidation of methionine, acetylation of the protein N-terminus, methionine loss, and methionine loss with acetylation were specified as variable modifications. The false discovery rate (FDR) for proteins, peptides, and PSMs was adjusted to be less than 1% [24].

ELISA

Serum levels of PGR4, PCYOX1, IGFBP3, APOM, CSF1R, FN1, ZG16, FETUB, MANF, LY6D, F9, SVEP1, and ADAMTSL1 were quantified using commercial ELISA kits from FineTest (Wuhan, China; PGR4: Cat No.EH1094; PCYOX1: Cat No.EH10957; IGFBP3: Cat No.EH0169; APOM: Cat No.EH2134; CSF1R: Cat No.EH3341; FN1: Cat No.EH0134; ZG16: Cat No.EH2154; FETUB: Cat No.EH3055; MANF: Cat No.EH3322; LY6D: Cat No.EH9883; F9: Cat No.EH3031); ABclonal Technology (Wuhan, China; SVEP1: Cat No.RK12086); and Signalway Antibody (Maryland, USA; ADAMTSL1: Cat No.EK7713). The sample concentration was calculated on the basis of the standard curve according to the manufacturers' instructions.

Statistical analysis

Statistical analyses and graph plotting were conducted using GraphPad Prism 8.0 (GraphPad, La Jolla, CA, USA) software. Correlations among samples were evaluated with Pearson's correlation coefficient. Differences between groups were compared using unpaired Student's t tests and Welch's t tests. Receiver operating characteristic (ROC) curves were generated with the area under the curve (AUC) to show the diagnostic performance of the biomarkers. The optimal cut-off value for FN1 was ascertained from the ROC curve utilizing the Youden index. $P < 0.05$ was considered statistically significant.

Results

Study design and participants

The study design is outlined in Fig. 1. All patients were pathologically diagnosed and staged according to the American Joint Committee on Cancer (AJCC) staging system (8th edition). The age and sex distributions were balanced separately in the discovery stage and different validation stages. VCA-IgA titers were quantified in all groups (HCs, ENPC, and LNPC), while EBV DNA levels were additionally evaluated in ENPC and LNPC patients. The EBV DNA and VCA-IgA measurements are obtained from clinical case records. Detailed clinical information is presented in Table 1.

Proteomic characterization of serum samples

Firstly, serum protein candidates were discovered by a label-free LC–MS/MS approach based on 15 samples. By applying a 1% false discovery rate (FDR) criterion at the spectral, peptide, and protein levels, a total of 1364 proteins were quantified.

Quality control was conducted on the MS-derived data. The results revealed that the peptides predominantly exhibited 2–3 charges and lengths ranging from 7–20 amino acids, with most proteins corresponding to more than two peptides (Fig. 2A, B). Pearson's correlation coefficient (PCC) analysis was used to delineated the relationships between samples, with all the Pearson coefficients exceeding 0.95 (Fig. 2C). Principal component analysis (PCA) was performed to visualize differences in protein profiles, revealing a distinct clustering trend within each group (Fig. 2D). Both the PCC and PCA demonstrated strong correlations and excellent repeatability of the samples.

FN1 was identified as a novel serum protein biomarker

Differential proteins were classified into six clusters with similar expression profiles and biological pathways associated with NPC (Fig. 3). We focused our analysis on cluster 2 and cluster 3, which showed significant differences in expression between the ENPC and LNPC groups, with comparable levels in the HC and ENPC groups. The enrichment analysis revealed a similar trend in tumor-related functions, such as gap junction, apoptosis, and metabolism.

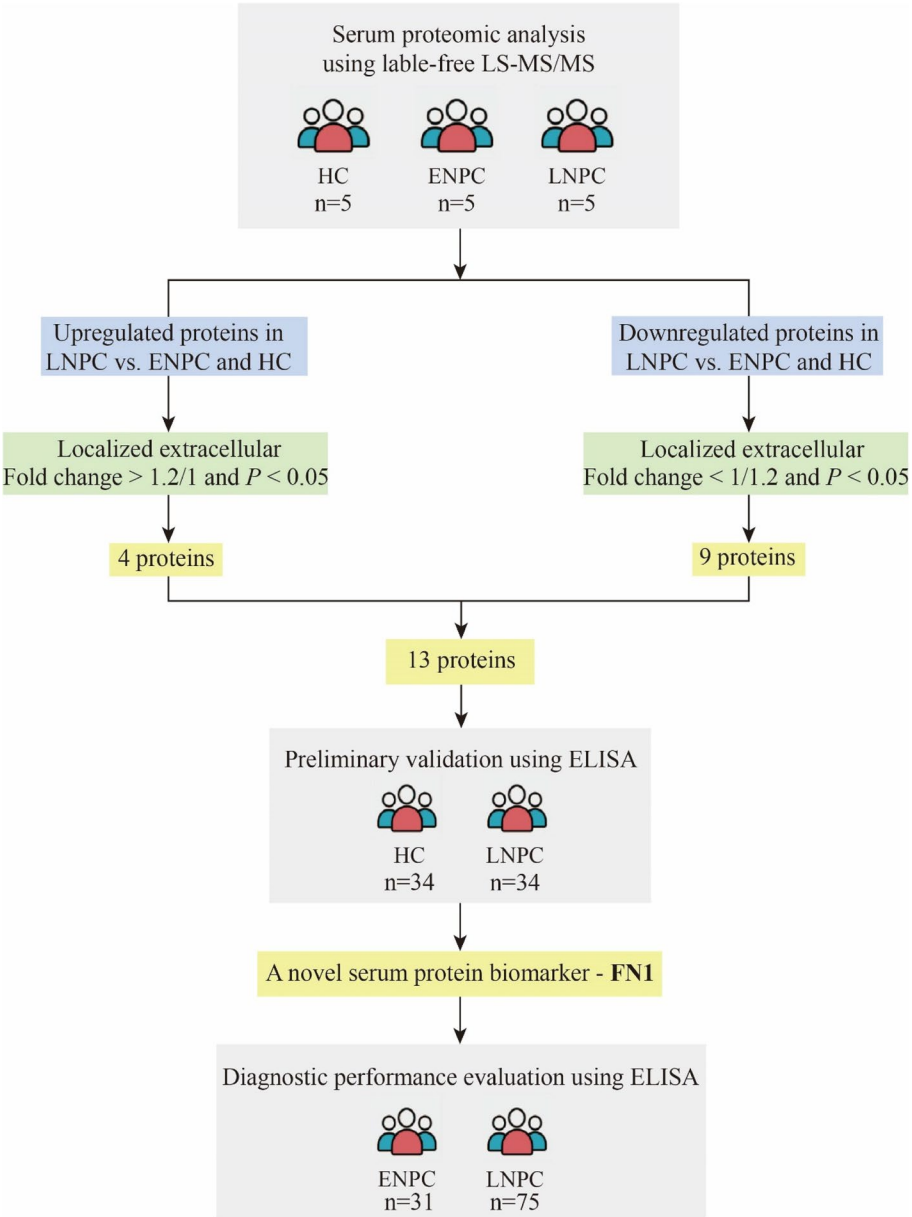

Fig. 1 Study design. The workflow of this study

In cluster 3, we identified 37 proteins that are localized extracellularly (Fig. 4A). Based on a criterion of a mean fold change less than 1/1.2 and a *P* value < 0.05 in both the LNPC/HC and LNPC/ENPC comparisons, 9 proteins were identified (Fig. 4B). Similarly, 4 proteins in cluster 2 were recognized with a mean fold change greater than 1.2/1 and a *P* value < 0.05 in the same comparisons (Supplementary Fig. 1A, B).

Given that early-stage NPC samples are relatively rare, as most patients are diagnosed at a late stage, we utilized commercial ELISA kits for preliminary validation in 34 HCs and 34 LNPC patients. As shown in Fig. 4C, the serum levels of FN1 ($P = 0.003$) were significantly lower in LNPC patients than in HCs. The levels of the remaining 12 proteins, PGR4, PCYOX1, IGFBP3, APOM, CSF1R, ZG16, FETUB, MANF, LY6D, F9, SVEP1 and ADAMTSL1, exhibited poor discriminatory performance (Fig. 4C and Supplementary Fig. 1C). These results revealed that FN1 is a potential biomarker associated with LNPC.

Table 1 Clinical information of the study participants in the discovery and validation stages

Characteristics	Discovery			Validation in HC and LNPC		Validation in ENPC and LNPC	
	HC($n=5$)	ENPC($n=5$)	LNPC($n=5$)	HC($n=34$)	LNPC($n=34$)	ENPC($n=31$)	LNPC($n=75$)
Age (years)							
Median	45	43	46	50	44	50	49
(min–max)	(35–53)	(33–52)	(34–60)	(40–64)	(6–67)	(33–65)	(25–71)
Sex							
Male	5	5	5	17	17	23	55
Female	0	0	0	17	17	8	20
VCA-IgA (1:X)							
+(≥1:40)	0	4	5	0	28	15	64
-(<1:40)	5	1	0	34	6	16	11
EBV DNA (copy/ml)							
+(≥100)	-	1	5	-	22	5	58
-(<100)	-	4	0	-	12	26	17

Diagnostic potential of FN1 in LNPC

Among these 68 samples, a FN1 concentration exceeding 147,695 ng/ml was considered positive, while a negative result was deemed significant. The AUC value for FN1 in discriminating LNPC patients from HCs was 0.71 (Fig. 5A, C). Concurrently, VCA-IgA exhibited a specificity of 100% by being negative in all HCs and demonstrated remarkable diagnostic accuracy, with an AUC of 0.96 (Fig. 5B, C, D). In the cohort of 34 LNPC patients, only 82.4% (28/34) of patients tested positive for VCA-IgA. Notably, FN1 accurately identified 3 additional LNPC patients who were VCA-IgA-negative (3/6), hinting that the combination of FN1 with VCA-IgA could increase the detection sensitivity and potentially decrease the misdiagnosis rate compared with VCA-IgA alone (Fig. 5D).

FN1 complemented VCA-IgA and EBV DNA in late-stage diagnosis

We evaluated the distinguishing effect of FN1 in 31 ENPC patients and 75 LNPC patients. Here, a FN1 concentration exceeding 216,689 ng/ml was defined as positive, while a negative result was deemed significant. The concentrations of FN1, VCA-IgA, and EBV DNA all showed statistically significant differences between the ENPC and LNPC groups (Fig. 6A, B, C). Among these, EBV DNA achieved a sensitivity, specificity, and AUC of 77.3%, 83.9%, and 0.82, respectively, whereas VCA-IgA yielded a sensitivity, specificity, and AUC of 85.3%, 51.6%, and 0.73, respectively. Although EBV DNA shows no strong sensitivity to VCA-IgA, its specificity is significantly higher than that of VCA-IgA. Therefore, EBV DNA demonstrates better diagnostic performance for late-stage NPC. However, the combined use of FN1, VCA-IgA, and EBV DNA resulted in an AUC of only 0.83 (Fig. 6D).

When patients were stratified by VCA-IgA results, FN1 could yield diagnostic power in the groups of VCA-IgA-negative and -positive patients, with AUCs of 0.71 and 0.80, respectively (Fig. 7A, B, C). Similarly, when patients were stratified by EBV DNA levels, FN1 achieved AUCs of 0.70 and 0.87 in distinguishing early- or late-stage NPC, respectively (Fig. 7D, E, F).

Among the 75 LNPC patients, 64 (85.3%) were VCA-IgA-positive. Notably, the remaining 11 patients with negative VCA-IgA results all had negative FN1 results. (Fig. 7G). EBV DNA correctly identified 77.3% (58/75) of LNPC patients, and we found that FN1 identified an additional 88.2% (15/17) of those who were EBV DNA-negative successfully (Fig. 7H). These findings suggest that FN1 could effectively enhance diagnostic sensitivity for LNPC patients with negative VCA-IgA or EBV DNA.

Additionally, we further explored the correlation between VCA-IgA and EBV DNA levels and found that they do not complement each other in late-stage NPC diagnosis (Supplementary Fig. 2A, B). Taken together, the findings of this study identify FN1 as a biomarker that provides a degree of complementarity with VCA-IgA and EBV DNA detection for the diagnosis of advanced NPC.

Discussion

Although globally rare, NPC is prevalent in Southern China, Southeast Asia, North Africa, and the Arctic [25]. The early stage of NPC often lacks specific clinical signs and syndromes, which increases the difficulty of diagnosis and raises the risk of misdiagnosis [26–28]. The AJCC 8th edition provides a staging system that categorizes NPC on the basis of tumor size and local invasion (T), the

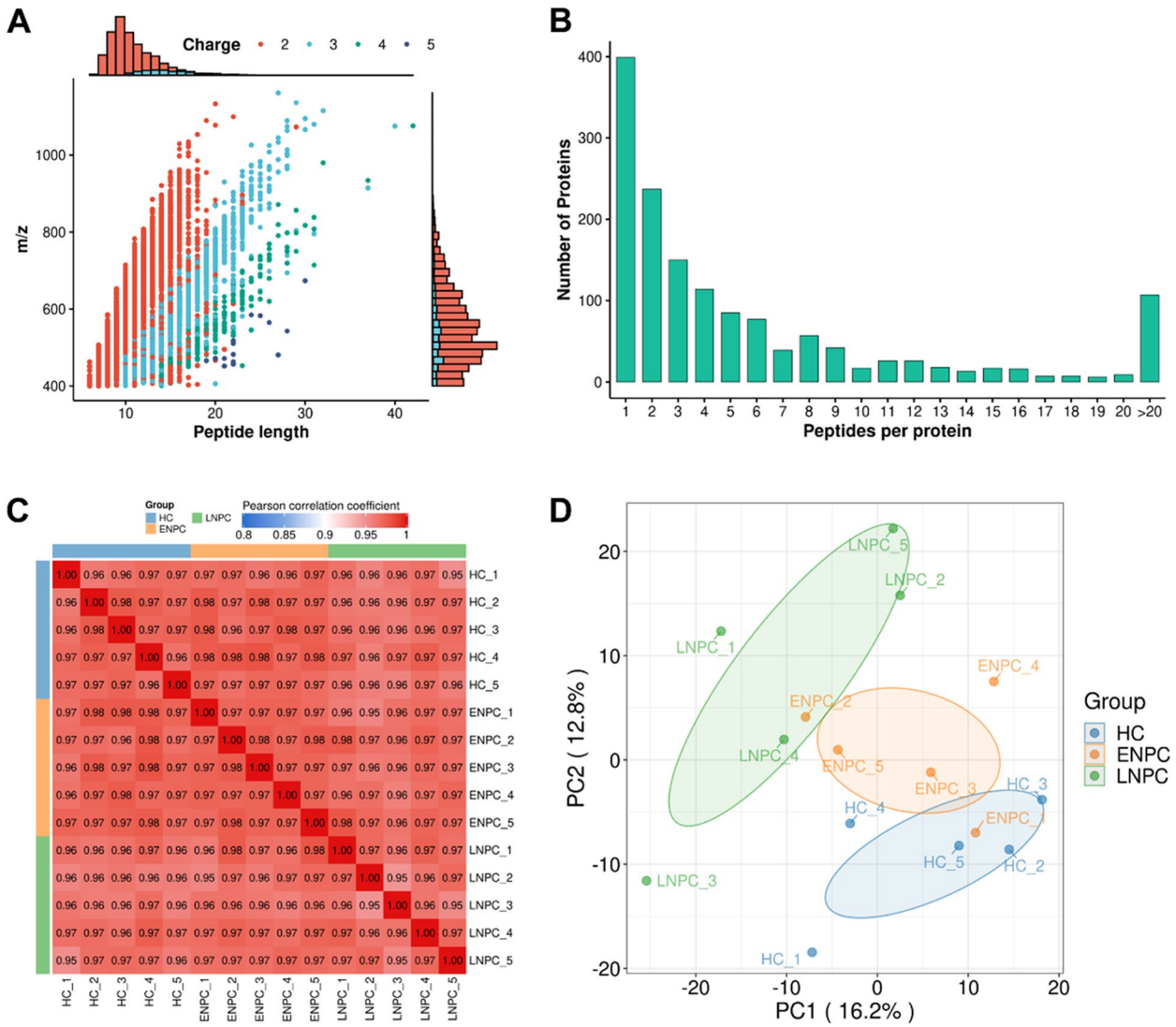

Fig. 2 Quantitative proteomics analysis. **A**. Plot of peptide length distribution. **B**. Plot of peptide number distribution. **C**. The correlation heatmap of 15 samples from the HC, ENPC and LNPC groups. **D**. Score plot of principal component analysis (PCA) among the HC, ENPC and LNPC groups

involvement of regional lymph nodes (N), and the presence of distant metastasis (M). Early-stage NPC (stage I and II) is characterized by tumors that are confined to the nasopharynx (T1-2) without extensive local invasion, and with no cervical lymph node involvement (N0) or minimal involvement (N1). These patients typically have a more favorable prognosis and often respond well to radiotherapy alone. In contrast, late-stage NPC (stage III and IV) presents with tumors that extend beyond the nasopharynx (T3-4), involve cervical lymph nodes more extensively (N2-3), or exhibit distant metastasis (M1). Late-stage NPC always necessitates a multimodal therapeutic approach, including concurrent chemoradiotherapy, induction chemotherapy followed by radiotherapy, and possibly targeted therapies or immunotherapy, which places a tremendous burden on both life and the economy. Therefore, accurately identifying late-stage NPC is essential for appropriate treatment strategies, which can significantly impact patient survival and quality of life.

Serum, an essential component of body fluids, plays an essential role in maintaining normal material transport, signal transduction, and immune defense. Serum proteins not only reflect primary tumor signals but also indicate potential micro-metastases post-treatment, as well as host inflammatory and immune responses [29, 30]. In this study, we systematically analyzed serum proteins through high-throughput quantitative proteomic technology, leading to the discovery of a novel biomarker.

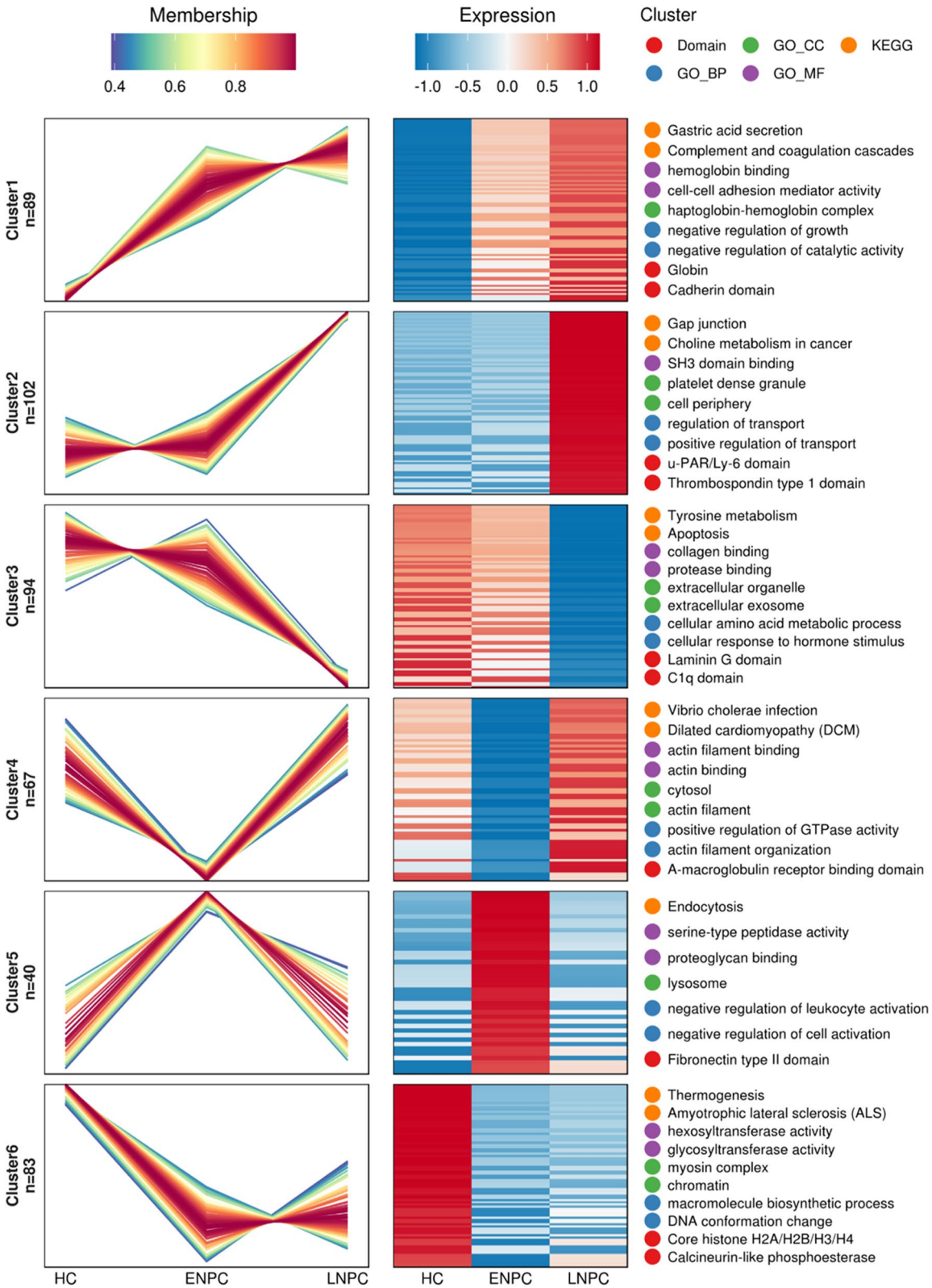

Fig. 3 Differential proteins were categorized by cluster analysis. Proteins with similar expression patterns and pathways or functions related to NPC were grouped into 6 clusters

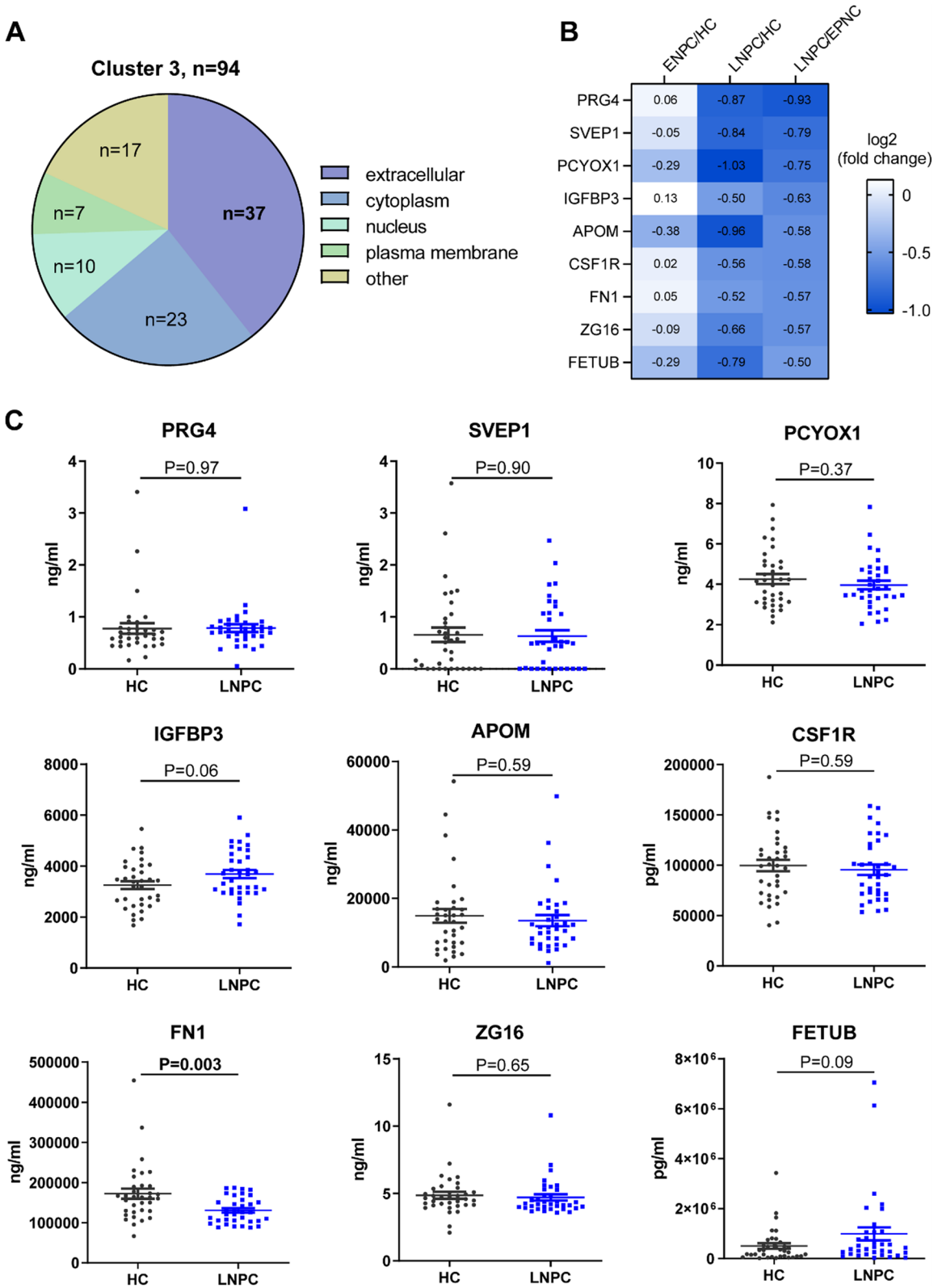

Fig. 4 Identification of serum protein biomarkers. **A**. Pie chart of the subcellular localization of 94 proteins in cluster 3. **B**. Log2 (fold change) values of PGR4, SVEP1, PCYOX1, IGFBP3, APOM, CSF1R, FN1, ZG16 and FETUB in the ENPC/HC, LNPC/HC and LNPC/ENPC comparisons. **C**. Scatter plot of PGR4, SVEP1, PCYOX1, IGFBP3, APOM, CSF1R, FN1, ZG16 and FETUB in 34 HCs and 34 LNPC patients. The centerline of each group represents the median value, and each dot represents a data point for an individual sample. The differences were analyzed by unpaired Student's t test

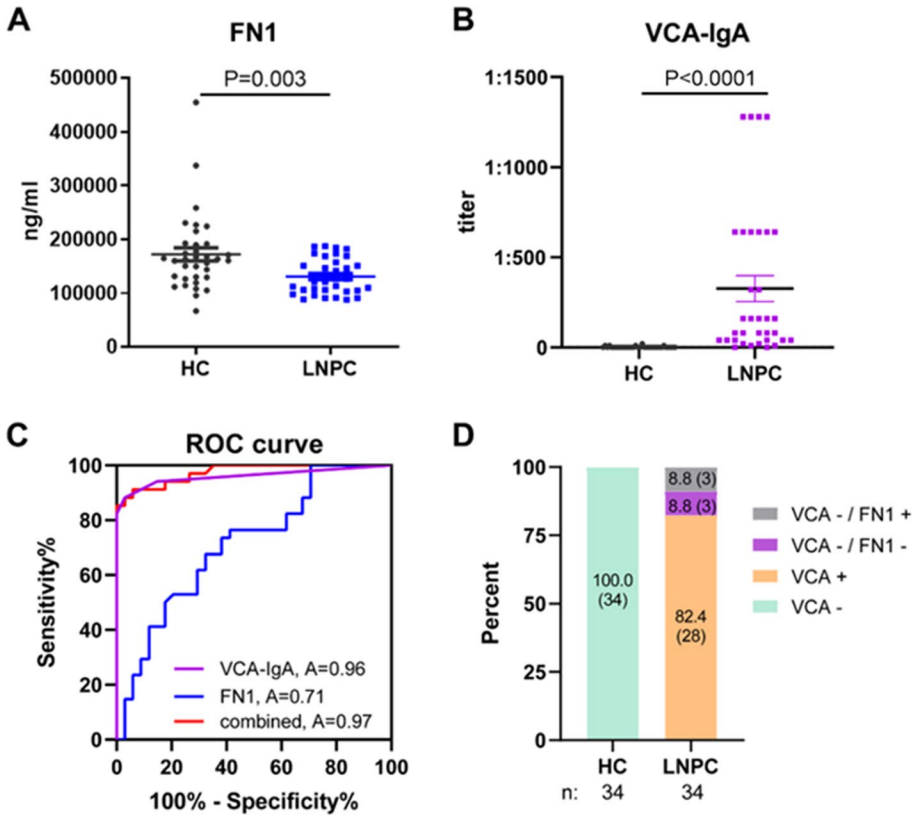

Fig. 5 Preliminary validation of FN1. **A**. Scatter plot of FN1 in the HC and LNPC groups. **B**. Scatter plot of VCA-IgA in the HC and LNPC groups. **C**. ROC curves of VCA-IgA, FN1, and their combination in the HC and LNPC groups. **D**. Diagnostic power of FN1 in individuals who were misdiagnosed by VCA-IgA. The values in parentheses indicate the number of samples corresponding to each percentage. +, positive; −, negative; n, number of samples. **A**, **B**. The centerline of each group represents the median value, and each dot represents a data point for an individual sample. **B**. The differences were analyzed by Welch's t test

In recent years, clinical practice has relied heavily on computed tomography (CT) and MRI as the principal diagnostic tools for evaluating the progression of NPC. Despite their pivotal role, these imaging modalities present several challenges, including high costs, limited sensitivity for detecting small lymph nodes, and contraindications for patients with renal insufficiency or a history of organ transplantation [31–33]. VCA-IgA and EBV DNA are established biomarkers for NPC. VCA-IgA targets the viral capsid antigen, which is expressed during the late phase of the EBV lytic cycle. Consequently, active viral replication or increased lymph node metastases are associated with elevated levels of VCA-IgA. The majority of studies have demonstrated a positive correlation between VCA-IgA titers and the N stage of NPC [34–36]. The detection of the EBV DNA load is also crucial in the diagnosis of NPC. Research has shown a correlation between the levels of EBV DNA and TNM stages, with stage I exhibiting the lowest levels and stage IV the highest [37]. Moreover, EBV DNA is particularly valuable for the diagnosis of stage III and IV, demonstrating high diagnostic capacity in advanced stages of NPC.

Current research on serum biomarkers for head and neck cancer, including NPC, like microRNA and exosomes, has primarily focused on early-stage diagnosis [38, 39]. However, our study introduces a novel perspective by emphasizing the diagnostic value of FN1 in late-stage NPC. The average level of FN1 in the serum of late-stage NPC patients was higher than 100 μg/ml, making it a reliable and practical biomarker for clinical application.

Based on the role of VCA-IgA and EBV DNA, we found that FN1 exhibits robust diagnostic capacity, particularly in LNPC patients who are negative for VCA-IgA and EBV DNA. The combination of FN1 with VCA-IgA or EBV DNA significantly enhances the diagnostic sensitivity, which could reduce the rate of false negatives and improve the overall diagnostic accuracy for late-stage NPC. Thus, we advocate for the incorporation of FN1 testing following VCA-IgA and EBV DNA detection. Importantly, VCA-IgA and EBV DNA do not provide

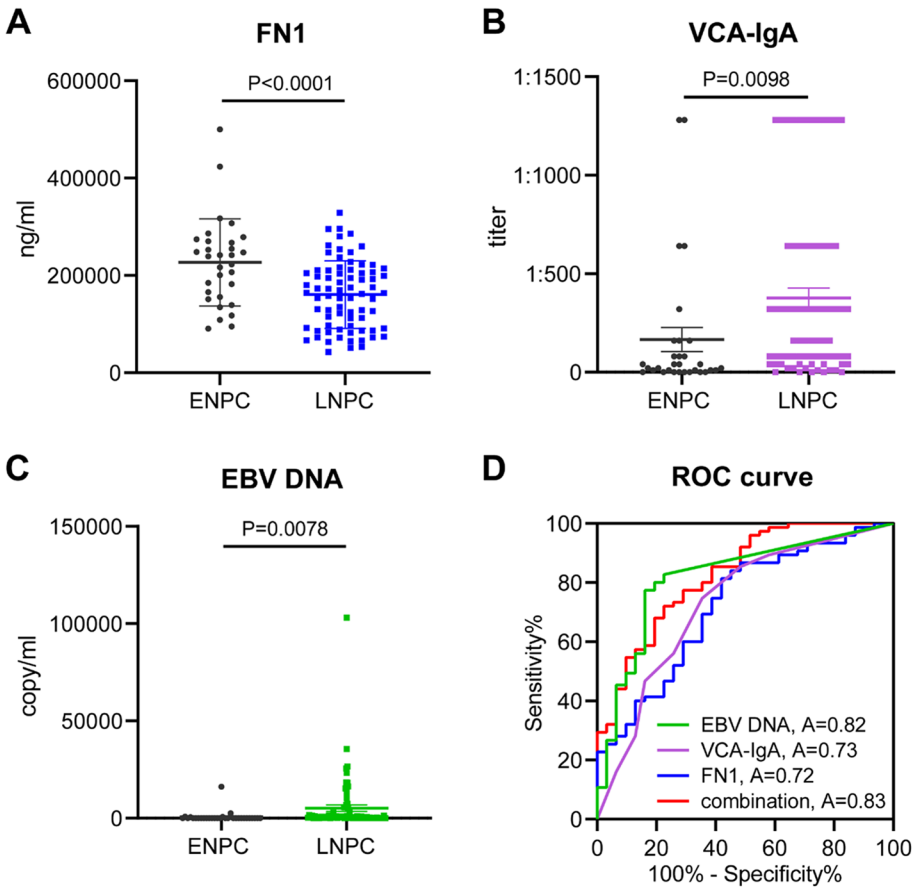

Fig. 6 Performance of FN1, VCA-IgA and EBV DNA in late-stage diagnosis. **A**. Scatter plot of FN1 in the ENPC and LNPC groups. The differences were analyzed by unpaired Student's t-test. **B**. Scatter plot of VCA-IgA in the ENPC and LNPC groups. **C**. Scatter plot of EBV DNA in the ENPC and LNPC groups. **A**, **B**, **C**. The centerline of each group represents the median value, and each dot represents a data point for an individual sample. **B**, **C**. The differences were analyzed by Welch's t test. **D**. ROC curves of EBV DNA, VCA-IgA, FN1, and their combination in the ENPC and LNPC groups

mutual supplementation in the diagnosis of late-stage NPC, likely because of their association with EBV infection. This highlights the unique potential of FN1 as a complementary diagnostic biomarker.

FN1 is an extracellular matrix (ECM) glycoprotein belonging to the fibronectin family and is widely distributed in cell structures such as smooth muscle cell layer, vascular cell membrane and nerve cell layer [40]. The function and correlation between FN1 expression and cancer incidence have been explored in various malignant tumors. FN1-induced alterations in gene expression are involved in multiple tumor biological behaviors [41]. The overexpression of FN1 has been observed in a variety of malignancies and may contribute to tumor metastasis and progression. Previous studies have shown that the upregulation of FN1 in tumor tissues is associated with poor prognosis in patients with gastric cancer [42, 43]. The migration and invasion of cancer cells in colon cancer and clear cell renal cell carcinoma are also known to be promoted by FN1 [44, 45]. Additionally, in patients with hepatocellular carcinoma and thyroid cancer, serum FN1 levels are significantly higher than those with non-neoplastic conditions, such as chronic liver inflammation and benign thyroid nodules [46, 47]. However, the relationship between serum FN1 levels and the progression of NPC remains unclear.

In this study, we found that the expression levels of FN1 in serum decreased with tumor progression, which contrasts with most of the clinical biomarkers. Some studies have identified serum proteins with decreased levels that serve as diagnostic or prognostic markers for various diseases, including CD248 for the early diagnosis of systemic lupus erythematosus, Apo A-I for the staging of hepatoblastoma and leukemia, and Valosin-containing human protein (VCP) for the prediction of preclinical and early clinical stages of Parkinson's disease [48–50]. This phenomenon may be attributed to ECM remodeling and the secretion of specific proteolytic enzymes [51, 52]. However, further investigations are needed to elucidate the underlying molecular mechanisms of FN1 and

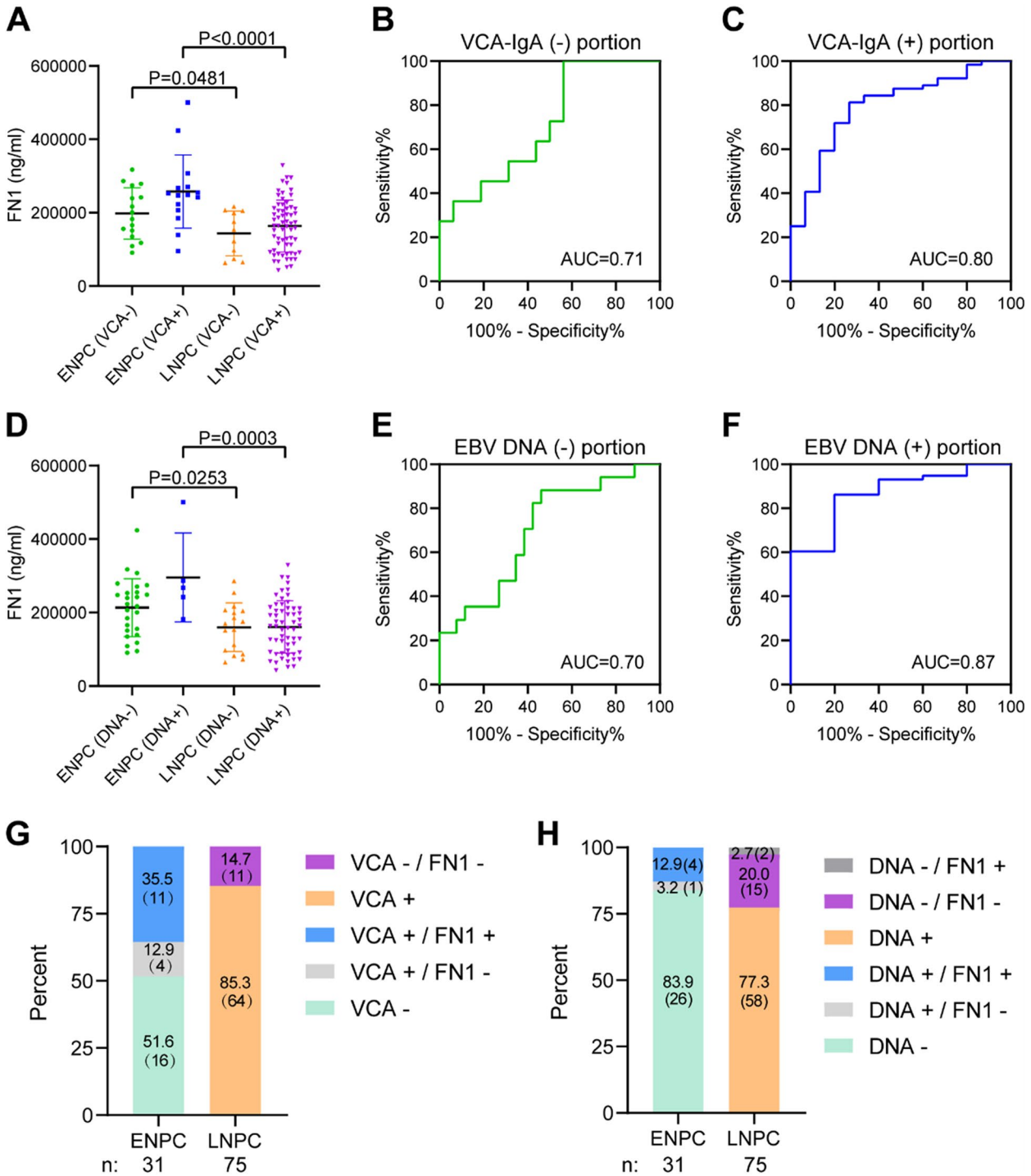

Fig. 7 Performance of FN1 in patients with different VCA-IgA or EBV DNA levels. **A**. Statistical significance of FN1 expression in the VCA-IgA-negative and -positive groups. **B**. ROC curve of FN1 in the VCA-IgA-negative groups. **C**. ROC curve of FN1 in the VCA-IgA-positive groups. **D**. Statistical significance of FN1 expression in EBV DNA-negative and -positive groups. **E**. ROC curve of FN1 in the EBV DNA-negative groups. **F**. ROC curve of FN1 in the EBV DNA-positive groups. **G**. Diagnostic power of FN1 in individuals who were misdiagnosed by VCA-IgA. **H**. Diagnostic power of FN1 in individuals who were misdiagnosed by EBV DNA. **A**, **D**. The centerline of each group represents the median value, and each dot represents a data point for an individual sample. The differences were analyzed by unpaired Student's t test. **G**, **H**. The values in parentheses indicate the number of samples corresponding to each percentage. +, positive; −, negative; n, number of samples

determine whether its downregulation leads to the development of NPC.

Furthermore, according to the cluster analysis, FN1 is more suitable as a biomarker for late-stage NPC diagnosis. Nevertheless, its diagnostic value in early-stage NPC remains unclear. Therefore, it is necessary to explore the potential of FN1 in early-stage diagnosis and to investigate other biomarkers for NPC diagnosis in future research.

Our study has several limitations. Firstly, the exclusive use of ELISA kits for both the discovery and validation stages may introduce constraints on the interpretation of the results. Secondly, the sample size was relatively small, especially the number of ENPC patients. The difficulty in obtaining early-stage NPC samples prevented us from including ENPC samples in the preliminary validation. Thirdly, the validation of FN1 was conducted within a single-center setting, so external validation using multiple analytical techniques in large, multi-center samples is necessary to generalize the conclusions.

Conclusion

In conclusion, the identification of FN1 as a novel serum protein biomarker for the accurate diagnosis of late-stage NPC marks a significant advancement in the field. Our data indicate that FN1 could significantly increase the diagnostic sensitivity of late-stage NPC when used in combination with established biomarkers such as VCA-IgA and EBV DNA. Nonetheless, these results hold promise for improving clinical management strategies and patient outcomes, potentially contributing to the development of more effective diagnostic and therapeutic approaches in NPC.

Abbreviations

NPC	Nasopharyngeal carcinoma
EBV	Epstein-Barr virus
HC	Healthy control
ELISA	Enzyme-linked immunosorbent assay
FN1	Fibronectin 1
AUC	Area under curve
MRI	Magnetic resonance imaging
PET-CT	Positron emission tomography-computed tomography
ENPC	Early-stage nasopharyngeal carcinoma
LNPC	Late-stage nasopharyngeal carcinoma
BCA	Bicinchoninic acid
FASP	Filter-aided sample preparation
TEAB	Tetraethylammonium bromide
SPE	Solid phase extraction
UPLC	Ultra performance liquid chromatography
MS	Mass Spectrometry
HCD	Higher Energy Collisional Dissociation
NCE	Normalized collision energy
AGC	Automatic gain control
FDR	False discovery rate
PSM	Peptide spectral Match
PGR4	Proteoglycan 4
PCYOX1	Prenylcysteine Oxidase 1
IGFBP3	Insulin-like Growth Factor Binding Protein 3
APOM	Apolipoprotein M
CSF1R	Colony-stimulating factor 1 receptor
ZG16	Zymogen Granule Protein 16
FETUB	Fetuin B
MANF	Mesencephalic Astrocyte Derived Neurotrophic Factor
LY6D	Lymphocyte Antigen 6 Family Member D
F9	Coagulation factor IX
SVEP1	Sushi, von Willebrand factor type A, EGF and pentraxin domain containing 1
ADAMTSL1	A disintegrin and metalloproteinase with thrombospondin motifs-like 1
ROC	Receiver operating characteristic
AJCC	American Joint Committee on Cancer
PCC	Pearson's correlation coefficient
PCA	Principal component analysis
CT	Computed tomography
ECM	Extracellular matrix
CD248	Tumor Endothelial Marker 1
Apo A-I	Apolipoprotein A-I
VCP	Valosin-containing protein

Supplementary Information

The online version contains supplementary material available at https://doi.org/10.1186/s12885-025-13958-8.

Supplementary Material 1.

Acknowledgements

Thanks to all the volunteers and all the authors for their valuable contributions to this study.

Authors' contributions

Zhu.Q. and Xing.S. were responsible for the overall design and supervision of the study. Huang.Q. collected clinical serum samples and organized the data. Pan.Y. and Zhu.Q. conducted the experiments and analyzed the data. Pan.Y. wrote the main manuscript text. All the authors contributed to the article and approved the submitted version.

Funding

This research was supported financially by the National Natural Science Foundation of China (82202509), Shenzhen Science and Technology Program (RCBS20221008093104015) and Innovative Talents Program of the Eighth Affiliated Hospital, Sun Yat-sen University (YXYXCXRC202305).

Data availability

Data is provided within the manuscript or supplementary information files. Further inquiries can be directed to the corresponding authors.

Declarations

Ethics approval and consent to participate

This study was approved by the Institution Review Board of SYSUCC. All procedures were performed in line with the principles of the Declaration of Helsinki. Informed consent was waived by the Institution Review Board of SYSUCC.

Consent for publication

Not applicable.

Competing interests

The authors declare no competing interests.

Received: 23 December 2024 Accepted: 18 March 2025
Published online: 01 April 2025

References

1. Chua MLK, Wee JTS, Hui EP, Chan ATC. Nasopharyngeal carcinoma. Lancet. 2016;387(10022):1012–24.
2. Tang LL, Chen WQ, Xue WQ, He YQ, Zheng RS, Zeng YX, Jia WH. Global trends in incidence and mortality of nasopharyngeal carcinoma. Cancer Lett. 2016;374(1):22–30.
3. Lam WKJ, Chan JYK: Recent advances in the management of nasopharyngeal carcinoma. F1000Res 2018, 7.
4. Zhang LF, Li YH, Xie SH, Ling W, Chen SH, Liu Q, Huang QH, Cao SM. Incidence trend of nasopharyngeal carcinoma from 1987 to 2011 in Sihui County, Guangdong Province, South China: an age-period-cohort analysis. Chin J Cancer. 2015;34(8):350–7.
5. Kamran SC, Riaz N, Lee N. Nasopharyngeal carcinoma. Surg Oncol Clin N Am. 2015;24(3):547–61.
6. Liu Z, Chang ET, Liu Q, Cai Y, Zhang Z, Chen G, Huang QH, Xie SH, Cao SM, Shao JY, et al. Quantification of familial risk of nasopharyngeal carcinoma in a high-incidence area. Cancer. 2017;123(14):2716–25.
7. Lin S, Pan J, Han L, Guo Q, Hu C, Zong J, Zhang X, Lu JJ. Update report of nasopharyngeal carcinoma treated with reduced-volume intensity-modulated radiation therapy and hypothesis of the optimal margin. Radiother Oncol. 2014;110(3):385–9.
8. Liu YP, Lv X, Zou X, Hua YJ, You R, Yang Q, Xia L, Guo SY, Hu W, Zhang MX, et al. Minimally invasive surgery alone compared with intensity-modulated radiotherapy for primary stage I nasopharyngeal carcinoma. Cancer Commun (Lond). 2019;39(1):75.
9. Sun X, Su S, Chen C, Han F, Zhao C, Xiao W, Deng X, Huang S, Lin C, Lu T. Long-term outcomes of intensity-modulated radiotherapy for 868 patients with nasopharyngeal carcinoma: an analysis of survival and treatment toxicities. Radiother Oncol. 2014;110(3):398–403.
10. Liu Z, Chen Y, Su Y, Hu X, Peng X. Nasopharyngeal Carcinoma: Clinical Achievements and Considerations Among Treatment Options. Front Oncol. 2021;11: 635737.
11. Lee AW, Ma BB, Ng WT, Chan AT. Management of Nasopharyngeal Carcinoma: Current Practice and Future Perspective. J Clin Oncol. 2015;33(29):3356–64.
12. Liao XB, Mao YP, Liu LZ, Tang LL, Sun Y, Wang Y, Lin AH, Cui CY, Li L, Ma J. How does magnetic resonance imaging influence staging according to AJCC staging system for nasopharyngeal carcinoma compared with computed tomography? Int J Radiat Oncol Biol Phys. 2008;72(5):1368–77.
13. Chen WS, Li JJ, Hong L, Xing ZB, Wang F, Li CQ. Comparison of MRI, CT and 18F-FDG PET/CT in the diagnosis of local and metastatic of nasopharyngeal carcinomas: an updated meta analysis of clinical studies. Am J Transl Res. 2016;8(11):4532–47.
14. Peng H, Chen L, Tang LL, Li WF, Mao YP, Guo R, Zhang Y, Liu LZ, Tian L, Zhang X, et al. Significant value of (18)F-FDG-PET/CT in diagnosing small cervical lymph node metastases in patients with nasopharyngeal carcinoma treated with intensity-modulated radiotherapy. Chin J Cancer. 2017;36(1):95.
15. Ho CY, Chan KT, Chu PY. Comparison of narrow-band imaging and conventional nasopharyngoscopy for the screening of unaffected members of families with nasopharyngeal carcinoma. Eur Arch Otorhinolaryngol. 2013;270(9):2515–20.
16. Chen YP, Chan ATC, Le QT, Blanchard P, Sun Y, Ma J. Nasopharyngeal carcinoma. Lancet. 2019;394(10192):64–80.
17. Abdel Khalek Abdel Razek A, King A: MRI and CT of nasopharyngeal carcinoma. AJR Am J Roentgenol 2012, 198(1):11–18.
18. Tsao SW, Tsang CM, Lo KW: Epstein-Barr virus infection and nasopharyngeal carcinoma. Philos Trans R Soc Lond B Biol Sci 2017, 372(1732).
19. Deng H, Zeng Y, Lei Y, Zhao Z, Wang P, Li B, Pi Z, Tan B, Zheng Y, Pan W, et al. Serological survey of nasopharyngeal carcinoma in 21 cities of south China. Chin Med J (Engl). 1995;108(4):300–3.
20. Chan KCA, Chu SWI, Lo YMD. Ambient Temperature and Screening for Nasopharyngeal Cancer. N Engl J Med. 2018;378(10):962–3.
21. Li WF, Zhang Y, Huang XB, Du XJ, Tang LL, Chen L, Peng H, Guo R, Sun Y, Ma J. Prognostic value of plasma Epstein-Barr virus DNA level during posttreatment follow-up in the patients with nasopharyngeal carcinoma having undergone intensity-modulated radiotherapy. Chin J Cancer. 2017;36(1):87.
22. Kim KY, Le QT, Yom SS, Ng RHW, Chan KCA, Bratman SV, Welch JJ, Divi RL, Petryshyn RA, Conley BA. Clinical Utility of Epstein-Barr Virus DNA Testing in the Treatment of Nasopharyngeal Carcinoma Patients. Int J Radiat Oncol Biol Phys. 2017;98(5):996–1001.
23. Wiśniewski JR, Zougman A, Nagaraj N, Mann M. Universal sample preparation method for proteome analysis. Nat Methods. 2009;6(5):359–62.
24. Käll L, Storey JD, MacCoss MJ, Noble WS. Assigning significance to peptides identified by tandem mass spectrometry using decoy databases. J Proteome Res. 2008;7(1):29–34.
25. Bray F, Ferlay J, Soerjomataram I, Siegel RL, Torre LA, Jemal A. Global cancer statistics 2018: GLOBOCAN estimates of incidence and mortality worldwide for 36 cancers in 185 countries. CA Cancer J Clin. 2018;68(6):394–424.
26. Lee AW, Sze WM, Au JS, Leung SF, Leung TW, Chua DT, Zee BC, Law SC, Teo PM, Tung SY, et al. Treatment results for nasopharyngeal carcinoma in the modern era: the Hong Kong experience. Int J Radiat Oncol Biol Phys. 2005;61(4):1107–16.
27. Li YY, Chung GT, Lui VW, To KF, Ma BB, Chow C, Woo JK, Yip KY, Seo J, Hui EP, et al. Exome and genome sequencing of nasopharynx cancer identifies NF-κB pathway activating mutations. Nat Commun. 2017;8:14121.
28. Agulnik M, Epstein JB. Nasopharyngeal carcinoma: current management, future directions and dental implications. Oral Oncol. 2008;44(7):617–27.
29. Liu Z, Zhou Q, He L, Liao Z, Cha Y, Zhao H, Zheng W, Lu D, Yang S. Identification of energy metabolism anomalies and serum biomarkers in the progression of premature ovarian failure via extracellular vesicles' proteomic and metabolomic profiles. Reprod Biol Endocrinol. 2024;22(1):104.
30. Tan C, Qin G, Wang QQ, Li KM, Zhou YC, Yao SK. Comprehensive serum proteomics profiles and potential protein biomarkers for the early detection of advanced adenoma and colorectal cancer. World J Gastrointest Oncol. 2024;16(7):2971–87.
31. Zhu YL, Deng XL, Zhang XC, Tian L, Cui CY, Lei F, Xu GQ, Li HJ, Liu LZ, Ma HL. Predicting distant metastasis in nasopharyngeal carcinoma using gradient boosting tree model based on detailed magnetic resonance imaging reports. World J Radiol. 2024;16(6):203–10.
32. Chan SC, Yeh CH, Yen TC, Ng SH, Chang JT, Lin CY, Yen-Ming T, Fan KH, Huang BS, Hsu CL, et al. Clinical utility of simultaneous whole-body (18)F-FDG PET/MRI as a single-step imaging modality in the staging of primary nasopharyngeal carcinoma. Eur J Nucl Med Mol Imaging. 2018;45(8):1297–308.
33. Lee ES, Kim TS, Kim SK. Current status of optical imaging for evaluating lymph nodes and lymphatic system. Korean J Radiol. 2015;16(1):21–31.
34. Li Y, Wang K, Yin SK, Zheng HL, Min DL: Expression of Epstein-Barr virus antibodies EA-IgG, Rta-IgG, and VCA-IgA in nasopharyngeal carcinoma and their use in a combined diagnostic assay. Genet Mol Res 2016, 15(1).
35. Xia C, Zhu K, Zheng G. Expression of EBV antibody EA-IgA, Rta-IgG and VCA-IgA and SA in serum and the implication of combined assay in nasopharyngeal carcinoma diagnosis. Int J Clin Exp Pathol. 2015;8(12):16104–10.
36. Sun R, Wang X, Li X. Correlation Analysis of Nasopharyngeal Carcinoma TNM Staging with Serum EA IgA and VCA IgA in EBV and VEGF-C and -D. Med Sci Monit. 2015;21:2105–9.
37. Ji MF, Huang QH, Yu X, Liu Z, Li X, Zhang LF, Wang P, Xie SH, Rao HL, Fang F, et al. Evaluation of plasma Epstein-Barr virus DNA load to distinguish nasopharyngeal carcinoma patients from healthy high-risk populations in Southern China. Cancer. 2014;120(9):1353–60.
38. Lin C, Chen Y, Lin X, Peng H, Huang J, Lin S, Pan J, Li M, Zong J. Plasma Epstein-Barr virus microRNA BART8-3p as a potential biomarker for detection and prognostic prediction in early nasopharyngeal carcinoma. Sci Rep. 2024;14(1):7433.
39. Liu Y, Wen J, Huang W. Exosomes in nasopharyngeal carcinoma. Clin Chim Acta. 2021;523:355–64.
40. Zhou Y, Cao G, Cai H, Huang H, Zhu X: The effect and clinical significance of FN1 expression on biological functions of gastric cancer cells. Cell Mol Biol (Noisy-le-grand) 2020, 66(5):191–198.
41. Gao W, Liu Y, Qin R, Liu D, Feng Q. Silence of fibronectin 1 increases cisplatin sensitivity of non-small cell lung cancer cell line. Biochem Biophys Res Commun. 2016;476(1):35–41.
42. Ucaryilmaz Metin C, Ozcan G. Comprehensive bioinformatic analysis reveals a cancer-associated fibroblast gene signature as a poor prognostic factor and potential therapeutic target in gastric cancer. BMC Cancer. 2022;22(1):692.

43. Wang H, Zhang J, Li H, Yu H, Chen S, Liu S, Zhang C, He Y. FN1 is a prognostic biomarker and correlated with immune infiltrates in gastric cancers. Front Oncol. 2022;12: 918719.
44. Xie Y, Liu C, Qin Y, Chen J, Fang J. Knockdown of IRE1α suppresses metastatic potential of colon cancer cells through inhibiting FN1-Src/FAK-GTPases signaling. Int J Biochem Cell Biol. 2019;114: 105572.
45. Steffens S, Schrader AJ, Vetter G, Eggers H, Blasig H, Becker J, Kuczyk MA, Serth J. Fibronectin 1 protein expression in clear cell renal cell carcinoma. Oncol Lett. 2012;3(4):787–90.
46. Kim H, Park J, Kim Y, Sohn A, Yeo I, Jong YuS, Yoon JH, Park T, Kim Y. Serum fibronectin distinguishes the early stages of hepatocellular carcinoma. Sci Rep. 2017;7(1):9449.
47. Ye G, Zhang X, Li M, Lin Z, Xu Y, Dong H, Zhou J, Zhang J, Wang S, Zhu Y, et al. Integrated analysis of circulating and tissue proteomes reveals that fibronectin 1 is a potential biomarker in papillary thyroid cancer. BMC Cancer. 2023;23(1):412.
48. Zhou G, Wei P, Lan J, He Q, Guo F, Guo Y, Gu W, Xu T, Liu S. TMT-based quantitative proteomics analysis and potential serum protein biomarkers for systemic lupus erythematosus. Clin Chim Acta. 2022;534:43–9.
49. Zhao W, Li J, Zhang J, Gao P, Pei H, Wang L, Guo F, Yu J, Zheng S, Wang J. Detection of Serum Protein Biomarkers for the Diagnosis and Staging of Hepatoblastoma. Int J Mol Sci. 2015;16(6):12669–85.
50. Alieva A, Rudenok M, Filatova E, Karabanov A, Doronina O, Doronina K, Kolacheva A, Ugrumov M, Illarioshkin S, Slominsky P, et al. VCP expression decrease as a biomarker of preclinical and early clinical stages of Parkinson's disease. Sci Rep. 2020;10(1):827.
51. Mohan V, Das A, Sagi I. Emerging roles of ECM remodeling processes in cancer. Semin Cancer Biol. 2020;62:192–200.
52. Herszényi L, Barabás L, Hritz I, István G, Tulassay Z. Impact of proteolytic enzymes in colorectal cancer development and progression. World J Gastroenterol. 2014;20(37):13246–57.

Publisher's Note